materials proceedings

MDPI

Proceeding Paper

SERS Detection of Methylene Blue and Crystal Violet Using Silver Nanostars †

José Luis Zamora-Navarro [1], Daniela González-Zárate [1], Mario A. Díaz-Solís [2], María Guadalupe Soriano-Rosales [2], Yuri B. Okolodkov [3] and Luis Zamora-Peredo [2,*]

[1] Facultad de Ciencias Químicas, Región Veracruz, Universidad Veracruzana, Boca del Rio 94294, Mexico
[2] Centro de Investigación en Micro y Nanotecnología, Universidad Veracruzana, Boca del Rio 94294, Mexico
[3] Instituto de Ciencias Marinas y Pesquerías, Universidad Veracruzana, Boca del Rio 94290, Mexico
* Correspondence: luiszamora@uv.mx
† Presented at the 3rd International Online-Conference on Nanomaterials, 25 April–10 May 2022; Available online: https://iocn2022.sciforum.net/.

Abstract: In this work, silver nanostars were synthesized using silver nitrate, ascorbic acid and polyvinylpyrrolidone (PVP), where the concentration of PVP varied from 0.1 to 10 mM. The morphology was studied by scanning electron microscopy where it was observed that the diameter decreases as the PVP concentration decreases. By UV–Vis absorption measurements typical nanostar spectra were found. In addition, surface-enhanced Raman spectroscopy (SERS) substrates were fabricated by depositing silver nanostars over copper film to detect methylene blue and crystal violet. This study allowed us to identify nanostars as an excellent nanostructure for the fabrication of ultrasensitive SERS substrates for the detection of persistent organic pollutants.

Keywords: silver nanostars; SERS substrates; methylene blue; crystal violet

Citation: Zamora-Navarro, J.L.; González-Zárate, D.; Díaz-Solís, M.A.; Soriano-Rosales, M.G.; Okolodkov, Y.B.; Zamora-Peredo, L. SERS Detection of Methylene Blue and Crystal Violet Using Silver Nanostars. *Mater. Proc.* **2022**, *9*, 27. https://doi.org/10.3390/materproc2022009027

Academic Editor: Guanying Chen

Published: 24 April 2022

1. Introduction

Surface-enhanced Raman spectroscopy (SERS) detection with silver nanostars (AgNS) as substrates have been used to detect organic dyes [1–3], fungicides [4], pesticides [5], and molecules related to biological analytes [6] due to their better performance with hotspots that enhanced the Raman signal compared to other nanostructures [7–9]. Other applications for detection of DNA mutation [10], Levodopa (drugs essential for the medical treatment of Parkinson disease) [11] or a-Fetoprotein (biomarker associated with many cancer types) [12] illustrate the importance of the silver nanostars.

Verma et al. have reported that is possible to obtain the star morphology by chemical reduction of Ag^+ using silver nitrate ($AgNO_3$), L-ascorbic acid (L-AA) and polyvinylpyrrolidone (PVP) [2,13]. They investigated the influence of L-AA and PVP concentrations on the nanoparticle morphology using different [$AgNO_3$]:[L-AA] molar ratios (R1) ranging between 0.04 and 2 and [$AgNO_3$]:[PVP] molar ratios (R2) ranging between 2.5 and 50. In this work, silver nanostars were synthesized using silver nitrate, ascorbic acid and PVP with a constant molar ratio R1 of 0.05 and varying only the PVP molarity from 0.1 to 10 mM ($36 < R2 < 0.36$). The behavior of the morphology and size of the nanostars was studied with scanning electron microscopy and UV–Vis absorption. In addition, SERS substrates were fabricated by depositing silver nanostars over copper film to determine which morphology and size offered the lowest detection limit of methylene blue (MB) and crystal violet (CV). This study allowed us to identify nanostars as an excellent nanostructure for the fabrication of ultrasensitive SERS substrates for the detection of persistent organic pollutants.

2. Materials and Methods

2.1. Materials

Silver nitrate ($AgNO_3$, ≥99%), Polyvinylpyrrolidone (PVP, MW 40000, 99%), methylene blue (MB), and crystal violet (CV) were purchased from Sigma-Aldrich (Waltham, MA, USA). L-ascorbic acid (L-AA, 99.5%) was purchased from Fagalab. Deionized water was used to dissolve all reagents in all experiments. All materials used were of analytical grade and were used as received without any further purification.

2.2. Fabrication of Silver Nanostars

The colloidal suspensions of AgNS were prepared by chemical reduction of $AgNO_3$ in a single step using L-ascorbic acid (L-AA) as a reducing agent and PVP as a capping agent. A mixture of a 3.6 mM $AgNO_3$ solution and a 10–0.1 mM PVP solution (different relative concentrations of PVP were studied in this work as listed in Table 1) was subjected to magnetic stirring. Subsequently, a 71.5 mM L-AA solution was added dropwise to the mixture without stirring. The color of the final suspension changed from colorless to light grey; depending on the concentration of the PVP solution the gray color became lighter.

Table 1. Silver nitrate, L-ascorbic acid and PVP concentrations used for AgNS studied in this work (SP = spheric, ST = star).

$AgNO_3$ [mM]	L-AA [mM]	PVP [mM]	R1 [$AgNO_3$]/[L-AA]	R2 [$AgNO_3$]/[PVP]	Size [μm]	Morphology
3.6	71.5	10	0.05	0.36	0.43	SP
3.6	71.5	5	0.05	0.72	0.36	SP
3.6	71.5	1	0.05	3.60	1.21	ST
3.6	71.5	0.8	0.05	4.50	1.07	ST
3.6	71.5	0.6	0.05	6.00	1.00	ST
3.6	71.5	0.4	0.05	9.00	0.62	ST
3.6	71.5	0.1	0.05	36.00	0.39	ST

2.3. Fabrication of Ag NS-Based SERS Substrates

First, copper substrates with a 2 cm × 2 cm area were cleaned with ethanol, hydrochloric acid, acetone, and deionized water. After drying the substrates, they were added to the $AgNO_3$-PVP mixture at the same time as L-ascorbic acid was added drop-wise, causing the formation of silver nanostars on the surface of the copper substrates. After 18 h, the AgNS-copper substrates were cleaned with deionized water to remove only the excess silver that was not deposited on the substrate. Next, 500 μL of 1 μM CV solution was dropped onto the AgNS substrates that were then allowed to dry under ambient conditions for one hour. Finally, deionized water was again used to remove excess analyte.

2.4. Characterization

Surface morphology of AgNS samples was investigated with a JEOL JSM 7600F field-emission scanning electron microcope (SEM), the absorbance spectra were obtained with a UV-Vis spectrometer (Thermo Scientific, Genesys 50) and SERS measurements were evaluated using a confocal Raman microscope (Thermo Scientific, DRX) equipped with a laser with 532-nm wavelength and 10-mW power. The SERS measurement was carried out using a laser power of 10 mW and 3 s of collection time.

3. Results and Discussion

Figure 1 shows the absorbance spectra obtained for the AgNS solutions 18 hours after starting the reaction, where a wide peak centered at 420 nm is observed for higher PVP concentrations, which is characteristic of spheric nanoparticles [9,11,14]. As the PVP concentration decreases the wide peak disappears, and the absorbance spectra are transformed to a shape characteristic of nanostar morphology reported by other authors [4,7,10]. It is possible to see how the absorbance decreases as the PVP concentration decreases to below 1 mM.

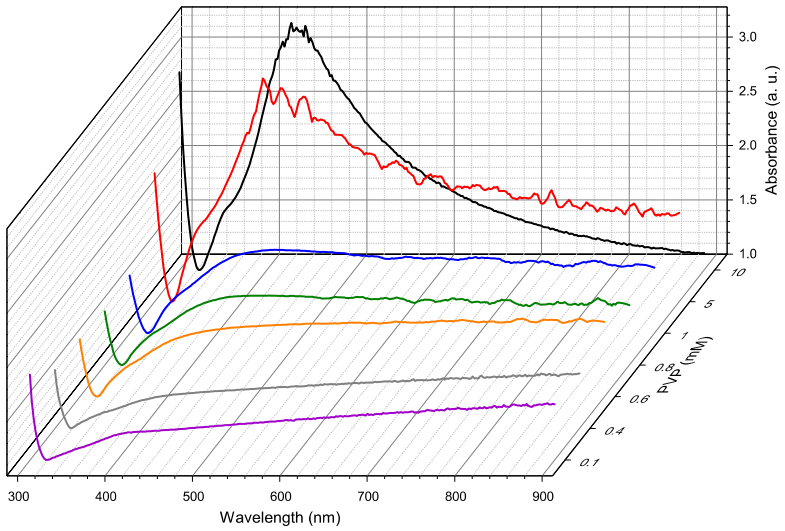

Figure 1. Absorbance spectra of Ag nanostars synthetized with 0.1, 0.4, 0.6, 0.8, 1.0, 5.0 and 10 mM PVP concentrations (violet, grey, orange, green, blue, red and black lines, respectively).

To explore the morphology of the AgNS, they were deposited on copper foil and then studied with a SEM. Figure 2 shows the SEM images of AgNS found for 5, 0.8, 0.6 and 0.4 mM PVP concentrations. These images are congruent with the absorbance spectra: at high PVP concentrations (5, 10) spherical nanoparticles are formed and, in contrast, at the lowest concentrations AgNS are obtained. Additionally, we found that the average diameter of the AgNS decreases as the PVP concentration decreases from 1.6 µm (1 mM) to 0.4 µm (0.1 mM); see Table 1.

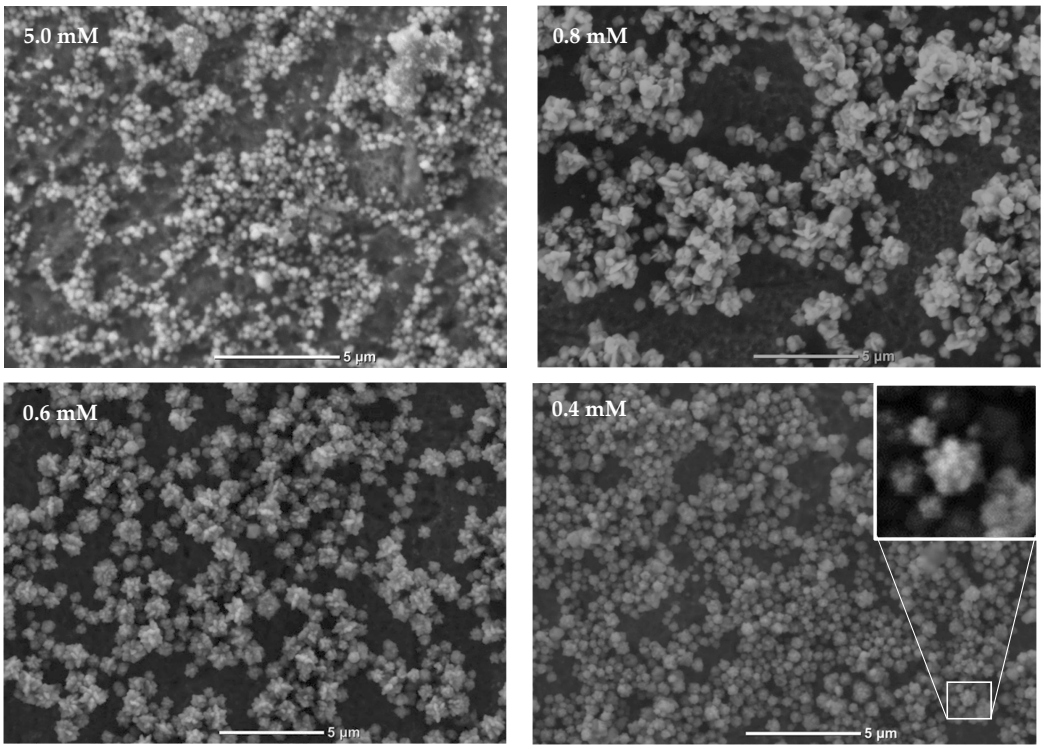

Figure 2. SEM micrographs of AgNS synthesized with different PVP concentrations, under constant the $AgNO_3$ and L-AA concentrations.

Considering absorption spectra and SEM images, is possible to establish that at the higher concentrations, PVP is adsorbed at full coverage on the Ag nanoparticles such that

smaller Ag spherical NP are formed. When the PVP concentration decreases, there is not enough PVP to saturate the surface of the AgNP such that preferential binding of PVP on Ag(100) facets explains the observed anisotropic growth along Ag(111) facets forming the Ag nanostars [15].

For MB detection, 0.5 mL of an aqueous solution with 10^{-6} mM of MB was deposited on the surface of AgNS/Cu-foil substrate and left for 1 h before Raman measurements. Figure 3a shows the SERS detection of MB by Ag nanostars at different PVP concentrations with two main peaks at 1436 cm^{-1} and 1620 cm^{-1}, respectively, associated with vibration modes ν_{asym} (C–N) and ν_{ring} (C–C) [16,17]. In Figure 3b the SERS intensity of the 1620 mode as a function of PVP concentration is plotted. A clear tendency is observed where the best detection of MB is with Ag nanostars synthesized at low PVP values.

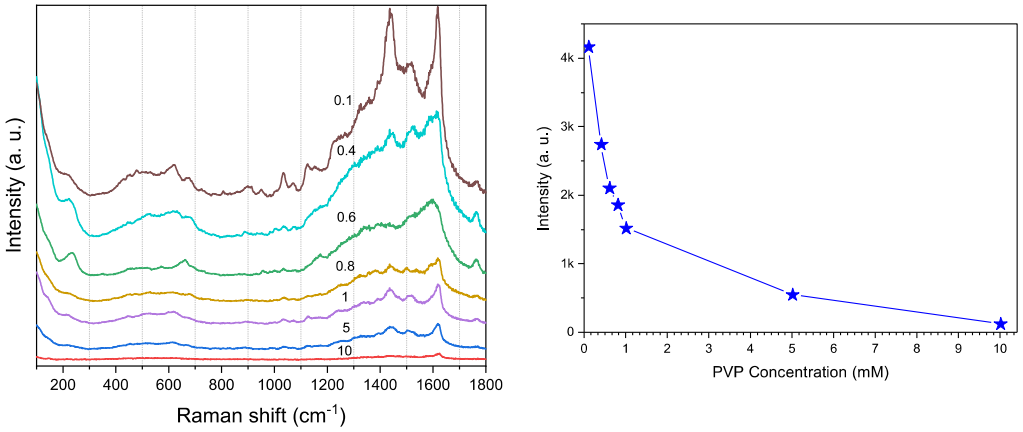

Figure 3. SERS detection of MB by Ag nanostars synthesized with different mM PVP concentrations (**a**) and SERS intensity of 1620 mode (**b**).

For CV detection, 0.5 mL of an aqueous solution with 10^{-6} mM of CV was deposited on the surface of AgNS/Cu-foil substrate and left for 1 h before Raman measurements. Figure 4a shows the SERS detection of CV by Ag nanostars at different PVP concentrations with easily observed peaks at 418, 439, 726, 804, 915, 1175, 1377, 1585 and 1618 cm^{-1}, associated with vibration modes of CV [18,19]. In Figure 4b the SERS intensity of the 1618 [ν_{ring} (C–C)] mode as a function of PVP concentration is plotted. The best SERS intensity of CV is with Ag nanostars synthesized at low PVP values, similar to that observed for MB.

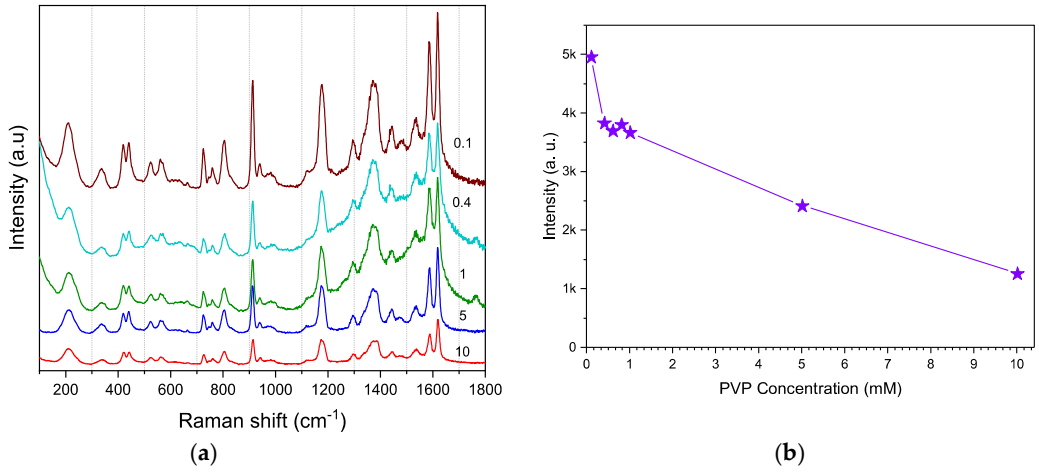

Figure 4. SERS detection of CV by Ag nanostars synthesized with different mM PVP concentrations (**a**) and SERS intensity of 1618 mode (**b**).

The best performance of SERS detection of MB and CV by AgNS synthesized with low PVP concentrations can be associated with the star morphology and the smaller diameters of nanoparticles obtained, suggesting that surface/volume ratio has been maximized.

4. Conclusions

Silver nanostars were synthesized using $AgNO_3$, L-AA and PVP. The molar ratio R1 ($AgNO_3$/L-AA) was fixed at 0.05 and the molar ratio R2 ($AgNO_3$/PVP) ranged between 0.36 and 36 (varying the PVP concentration from 10 to 0.1 mM). Ag spherical nanoparticles were observed at high PVP values, and conversely, Ag nanostars were found at low concentrations. The best performance of SERS detection of methylene blue and crystal violet was observed by AgNS synthesized with low PVP concentrations.

Author Contributions: Conceptualization and Planning, Research, Literature search, Writing—original draft preparation, J.L.Z.-N.; Research, D.G.-Z., M.G.S.-R. and M.A.D.-S.; Writing—review and editing, Y.B.O.; Conceptualization and planning, Writing—review, editing, revision, supervision, L.Z.-P. All authors have read and agreed to the published version of the manuscript.

Funding: This research received no external funding.

Institutional Review Board Statement: Not applicable.

Informed Consent Statement: Not applicable.

Data Availability Statement: This study did not report any data.

Acknowledgments: The authors would like to thank Marcia M. Gowing from Seattle, WA, USA, who kindly improved the writing style.

Conflicts of Interest: The authors declare no conflict of interest.

References

1. Oliveira, M.J.; Quaresma, P.; de Almeida, M.P.; Araújo, A.; Pereira, E.; Fortunato, E.; Martins, R.; Franco, R.; Águas, H. Office paper decorated with silver nanostars—An alternative cost effective platform for trace analyte detection by SERS. *Sci. Rep.* **2017**, *7*, 2480. [CrossRef] [PubMed]
2. Garcia-Leis, A.; Rivera-Arreba, I.; Sanchez-Cortes, S. Morphological tuning of plasmonic silver nanostars by controlling the nanoparticle growth mechanism: Application in the SERS detection of the amyloid marker Congo Red. *Colloids Surf. A Physicochem. Eng. Asp.* **2017**, *535*, 49–60. [CrossRef]
3. Zalaffi, M.S.; Agostinelli, I.; Karimian, N.; Ugo, P. Ag-nanostars for the sensitive SERS detection of dyes in artistic cross-sections—Madonna della Misericordia of the National Gallery of Parma: A case study. *Heritage* **2020**, *3*, 1344–1359. [CrossRef]
4. Verma, A.K.; Soni, R.K. Silver nanodendrites for ultralow detection of thiram based on surface-enhanced Raman spectroscopy. *Nanotechnology* **2019**, *30*, 385502. [CrossRef] [PubMed]
5. Sitjar, J.; Liao, J.-D.; Lee, H.; Pan, L.P.; Liu, B.H.; Fu, W.-E.; Chen, G.D. Ag Nanostructures with spikes on adhesive tape as a flexible SERS-active substrate for in situ trace detection of pesticides on fruit skin. *Nanomaterials* **2019**, *9*, 1750. [CrossRef] [PubMed]
6. Revnic, R.N.; Știufiuc, G.F.; Toma, V.; Onaciu, A.; Moldovan, A.; Țigu, A.B.; Fischer-Fodor, E.; Tetean, R.; Burzo, E.; Știufiuc, R.I. Facile microwave assisted synthesis of silver nanostars for ultrasensitive detection of biological analytes by SERS. *Int. J. Mol. Sci.* **2022**, *23*, 8830. [CrossRef] [PubMed]
7. Garcia-Leis, A.; Garcia-Ramos, J.V.; Sanchez-Cortes, S. Silver nanostars with high SERS performance. *J. Phys. Chem. C* **2013**, *117*, 7791–7795. [CrossRef]
8. Mosier-Boss, P.A. Review of SERS substrates for chemical sensing. *Nanomaterials* **2017**, *7*, 142. [CrossRef] [PubMed]
9. Zalaffi, M.S.; Litti, L.; Canton, P.; Meneghetti, M.; Moretto, L.M.; Ugo, P. Preparation and characterization of Ag-nanostars@Au-nanowires hierarchical nanostructures for highly sensitive surface enhanced Raman spectroscopy. *Nano Express* **2020**, *1*, 020006. [CrossRef]
10. Liu, Y.; Lyu, N.; Rajendran, V.K.; Piper, J.; Rodger, A.; Wang, Y. Sensitive and direct DNA mutation detection by surface-enhanced Raman spectroscopy using rational designed and tunable plasmonic nanostructures. *Anal. Chem.* **2020**, *92*, 5708–5716. [CrossRef] [PubMed]
11. Rubira, R.J.G.; Camacho, S.A.; Martin, C.S.; Mejía-Salazar, J.R.; Gómez, F.R.; da Silva, R.R.; Junior, O.N.D.O.; Alessio, P.; Constantino, C.J.L. Designing silver nanoparticles for detecting Levodopa (3,4-Dihydroxyphenylalanine, L-Dopa) using surface-enhanced Raman scattering (SERS). *Sensors* **2020**, *20*, 15. [CrossRef] [PubMed]
12. Zhao, J.; Wu, C.; Zhai, L.P.; Shi, X.F.; Li, X.; Weng, G.J.; Zhu, J.; Li, J.J.; Zhao, J.-W. A SERS-based immunoassay for the detection of α-fetoprotein using AuNS@Ag@SiO_2 core–shell nanostars. *J. Mater. Chem. C* **2019**, *7*, 8432–8441. [CrossRef]

13. Verma, A.K.; Soni, R.K. Multi-spiked silver stars for ultrasensitive and multiplexed SERS detection of analytes. *J. Phys. D Appl. Phys.* **2021**, *54*, 15. [CrossRef]
14. Qin, Y.; Ji, X.; Jing, J.; Liu, H.; Wu, H.; Yang, W. Size control over spherical silver nanoparticles by ascorbic acid reduction. *Colloids Surf. A Physicochem. Eng. Asp.* **2010**, *372*, 172–176. [CrossRef]
15. Chen, Z.; Chang, J.W.; Balasanthiran, C.; Milner, S.T.; Rioux, R.M. Anisotropic growth of silver nanoparticles is kinetically controlled by polyvinylpyrrolidone binding. *J. Am. Chem. Soc.* **2019**, *141*, 4328–4337. [CrossRef] [PubMed]
16. Li, C.; Huang, Y.; Lai, K.; Rasco, B.A.; Fan, Y. Analysis of trace methylene blue in fish muscles using ultra-sensitive surface-enhanced Raman spectroscopy. *Food Control* **2016**, *65*, 99–105. [CrossRef]
17. Nardo, V.M.; Renda, V.; Trusso, S.; Ponterio, R. Role of pH on nanostructured SERS active substrates for detection of organic dyes. *Molecules* **2021**, *26*, 2360. [CrossRef]
18. Shi, G.; Wang, M.; Zhu, Y.; Wang, Y.; Xu, H. A novel natural SERS system for crystal violet detection based on graphene oxide wrapped Ag micro-islands substrate fabricated from Lotus leaf as a template. *Appl. Surf. Sci.* **2018**, *459*, 802–811. [CrossRef]
19. Esenturk, E.N.; Walker, A.R.H. Surface-enhanced Raman scattering spectroscopy via gold nanostars. *J. Raman Spectrosc.* **2009**, *40*, 86–91. [CrossRef]